

# Charge Conservation and Higher Moments of Charge Fluctuations

Scott Pratt

*Department of Physics and Astronomy and National Superconducting Cyclotron Laboratory  
Michigan State University, East Lansing, MI 48824 USA*

Rachel Steinhorst

*Department of Physics and Astronomy  
Michigan State University, East Lansing, MI 48824 USA*  
(Dated: May 13, 2020)

## I. INTRODUCTION

The fluctuation of conserved charges is a standard means by which to investigate and gauge phase transitions. At the critical point correlation lengths diverge, which results in peaks in charge fluctuations as one approaches the critical point. For systems with first-order phase transitions, fluctuations become infinite whenever one is in a region of phase separation, as the liquid and gas regions prefer to become infinite in extent when the surface energy is non-zero. The growth of fluctuations becomes increasingly dramatic as one considers progressively higher-order fluctuations. In a volume  $V$ , fluctuations of a charge  $Q$  can be defined as

$$\mathcal{M}_N \equiv \frac{1}{V} \langle (Q - \bar{Q})^N \rangle = \frac{1}{V} \sum_n P_n (n - \bar{n})^N, \quad (1)$$

when particles have unit charge. The measure is increasingly sensitive to the tails of the multiplicity distribution,  $P_n$ , as  $N$  increases. The free energy,  $F \sim a_2(n - \bar{n})^2 + a_3(n - \bar{n})^3 \dots$ , is minimized for  $n = \bar{n}$ , but the quadratic part vanishes at the critical point,  $a_2 \rightarrow 0$ , which allows the fluctuations to grow and be dominated by higher-order terms which manifest themselves in the tails of the distribution.

The properties of the QCD transition, deconfinement and the restoration of chiral symmetry, are not well understood at finite baryon density. There exists the possibility that this transition is a true phase transition, with a critical point at several times nuclear density and with a critical temperature close to the pion mass. If this is the case, it begs the question as to whether the conditions for phase separation or for critical phenomena can be reproduced in the laboratory. Heavy ion collisions at high energy, measured at the Relativistic Heavy Ion Collider (RHIC) or at the LHC, can produce mesoscopic regions at temperatures of a few hundred MeV, which is well above the expectations for a critical temperature, and densities of several times nuclear matter density.

High-energy heavy ion collisions are characterized by strong explosive collective flow. Measurement is confined to the outgoing asymptotic momenta, but because of strong flow, correlations in coordinate space manifest themselves as correlations in relative momentum. Thus, measurements of correlations binned by relative momentum or charge fluctuations within some defined region of momentum space serve as surrogates for the corresponding observables in coordinate space. Indeed, measurements of charge and baryon number fluctuations have been performed at RHIC. By adjusting the beam energy of the colliding nuclei, experiments at RHIC have explored conditions at which novel phase phenomena might occur. Fluctuations of electric charge and baryon number have been especially popular. An initial scan of beam energies was rather inconclusive, but measurements with greatly improved statistics are currently being analyzed.

In addition to the finite system size (event multiplicities might number in the thousands), the novel states of matter created in heavy-ion collisions persist for  $\lesssim 10$  fm/c. This severely limits the degree to which phases can separate or to which critical fluctuations can grow. From the initial overlap of the colliding nuclei, until the mean time at which emitted particles experience their last collision, the collision lasts a few tens of fm/c. This limits the degree to which conserved charges can separate from one another. For example if a strange and an anti-strange quanta are produced together, their separation is limited by diffusion, and the enhancement of seeing a second charge of opposite sign having seen a first charge are known as charge-balance correlations.

The goal of this paper is to gauge the degree to which charge-balance correlations affect higher-order correlations. Such correlations need to be understood as potential sources of background before making firm arguments to have observed phenomena related to phase transitions. It is well known that charge-balance correlations are readily measurable at the two particle level,  $N = 2$  in Eq. (1), and that they explain the bulk of the  $N = 2$  fluctuation measurement. However, their impact on  $N = 3, 4$  fluctuations has not been investigated in great detail. For instance, the four-particle measure of correlation,

$$C_4 = \mathcal{M}_4 - 3\mathcal{M}_2^2, \quad (2)$$

which is based on cumulants, subtracts much of the contribution to the  $\mathcal{M}_4$  coming from purely two-particle correlations. However, charge conservation can involve multiple particles, and it is not clear the degree to which a cumulant-based measure, like the kurtosis, is affected by charge conservation. A simple model, where charge conservation is invoked through sampling a canonical ensemble, is presented in the next section. Although the method is different, this is similar to ideas that have been pursued recently [2]. But with the method used here, events can be generated in a more efficient algorithm, which then enables the more systematic set of studies presented here.

After a brief review of cumulants and the definitions of skewness and kurtosis in Sec. ??, the method for exact solution of the canonical ensemble describing a multi-component, multi-charge hadron gas is presented in Sec. ?. The method includes all species and can account for Bose or Fermi statistics, but neglects interaction between hadrons. These techniques extend those used for canonical ensembles used to study isospin fluctuations of a hadron gas [], nuclear fragmentation [], the level density of a Fermi gas, and the effect of restricting a quark-gluon plasma (QGP)

to having fixed charge, including being in an overall color singlet []. Exact methods for calculating correlations up to fourth-order are presented. Unfortunately, to include realistic acceptance effects and complex decays, the exact expressions are no longer viable. However, as shown in Sec. IV, the exact expressions show how sample events can be generated. An event, defined by a set of particles and momenta, are generated with perfect independence from one another, and perfectly reproduce the canonical expressions from Sec. III.

Conservation of charge is modeled by imagining independent sub-volume “patches” which individually conserve charge. The patch volume is set by how far charges have separated from another by the time chemical freezeout occurs, just after hadronization. After this time, the volumes may grow and overlap, but the chemical makeup of the particles originating from each patch is assumed to be fixed. Sections ?? and ?? shows how fluctuation observables from charge conservation depend of patch size, measurement efficiency, and the chemical decoupling temperature by investigating systems with fixed efficiency. A very simplified system with a single charge, as already investigated in detail in [], is reviewed in Sec. ??, while the full hadron gas, with three conserved charges, is presented in Sec. ??. The importance of Bose corrections for pions is also studied. Charge from the initial nuclei existed before the collision and might randomly populate the entire collision volume, whereas charge created from the breakup of color flux tubes, hadronization and decays, should be conserved locally. Thus, the effect of random placing some of the initial charge across the entire collision volume is also investigated. A more realistic picture of the acceptance and efficiency is presented in Sec. VII. A blast-wave model, which is a thermal model superimposed onto a simplified model of collective flow, is combined with a sampling of a canonical ensemble of a given patch. The resulting particles are then analyzed using a simulation of the acceptance and efficiency of the STAR Collaboration at RHIC. Results are compared to measurements at STAR to discern whether charge conservation effects might be responsible for a significant part of the observed correlation. Results are then summarized in Sec. VIII.

## II. CUMULANTS, SKEWNESS AND KURTOSIS

To keep the more manuscript self-contained, a brief review of cumulants and the definition of skewness and kurtosis is presented here.

Cumulants of a charge distribution are defined by

$$C_1 = \langle Q \rangle, \quad (3)$$

$$C_2 = \langle (Q - \bar{Q})^2 \rangle, \quad (4)$$

$$C_3 = \langle (Q - \bar{Q})^3 \rangle, \quad (5)$$

$$C_4 = \langle (Q - \bar{Q})^4 \rangle - C_2^2, \quad (6)$$

where  $Q$  is the net charge. Here,  $Q$  might refer to baryon number, to strangeness, or to the electric charge measured in units of  $e$ .

Rather than showing the cumulants  $C_n$ , ratios are presented to help minimize trivial dependences on system size. The skewness,  $S$ , is a measure of the third moment,

$$S = \frac{C_3}{C_2^{3/2}}. \quad (7)$$

This definition has the advantage in being dimensionless, but it does not become independent of volume in the limit of large volumes. Thus, it is more common to consider the ratio

$$S\sigma = S\sqrt{C_2} = \frac{C_3}{C_2}, \quad (8)$$

which becomes an intensive measure in the limit of larger volumes. The kurtosis is a measure of four-particle correlations,

$$K = \frac{C_4}{C_2^2}, \quad (9)$$

but instead of  $K$ , one typically chooses

$$K\sigma^2 = \frac{C_4}{C_2}, \quad (10)$$

to find an intensive measure of the fluctuation, at least for large volumes.

The measures  $S\sigma$  and  $K\sigma^2$  approach simple values in the limit that the distributions would be Poissonian. For Poissonian emission the observation of a charge in one region of momentum space is uncorrelated with the emission

into any other space. Thus, particles are correlated only with themselves. If charges appear only in integral positive units, one can apply the usual expression for the Poissonian moments where the mean is  $\eta$ ,

$$C_1 = \bar{n} = \eta \quad (11)$$

$$C_2 = \langle (n - \bar{n})^2 \rangle = \eta, \quad (12)$$

$$C_3 = \langle (n - \bar{n})^3 \rangle = \eta = C_1, \quad (13)$$

$$C_4 = \langle (n - \bar{n})^4 \rangle - 3C_2^2 = \eta. \quad (14)$$

If there exist both positive and negative charges, the distribution of the net charge can be derived by convoluting the two distributions. Convoluting two Poissonians results in a Skellam distribution. If the mean number of positives is  $\eta_+$  and the mean number of negatives is  $\eta_-$ , the distribution of net charge for a Skellam distribution,  $Q = n_+ - n_-$ , yields the following cumulants

$$C_1 = \eta_+ - \eta_-, \quad (15)$$

$$C_2 = \eta_+ + \eta_-, \quad (16)$$

$$C_3 = \eta_+ - \eta_- = C_1, \quad (17)$$

$$C_4 = \eta_+ + \eta_- = C_2. \quad (18)$$

Thus, if charges are produced in an uncorrelated fashion in increments of either  $\pm 1$ , the skewness and kurtosis become

$$S\sigma = \frac{C_3}{\sigma^2} = \frac{C_1}{\sigma^2}, \quad (19)$$

$$K\sigma^2 = \frac{C_4}{\sigma^2} = 1, \quad (20)$$

where  $\sigma^2 \equiv \langle (Q - \bar{Q})^2 \rangle = \eta_+ + \eta_-$ . It might have made more sense to consider  $C_3/C_1$  rather than  $S\sigma$ , as that ratio would be unity in the limit that emission is uncorrelated. However, because experimental analyses have often concentrated on the two ratios above, higher order correlations in this paper will also be presented in terms of these ratios.

Moments depend on the efficiency  $\alpha$  with which particles are measured. In the limit of vanishing efficiency all distributions of positives or of negatives tend to become Poissonian, and the distribution of the net charge will thus become a Skellam. This can be understood by having the probability of observing a positive charge being  $\alpha \rightarrow 0$  and the probability of observing two charges being proportional to  $\alpha^2$  being negligible. This assumption would fall through if all positive charges were measured in pairs, i.e. multiple charges on each measured particle, but for final-state hadrons the charges are only  $\pm 1$ . As  $\alpha \rightarrow 0$ , the moments are dominated by the probability of observing either zero charges or a single charge, and the moments for counting particles of a given charge are

$$\langle n^m \rangle = \alpha, \quad (21)$$

for all  $m > 0$ . It is then easy to see that  $\langle (n - \bar{n})^m \rangle = \alpha$ , which quickly leads to the result that as  $K\sigma^2 = C_3/C_1 = 1$ .

If the net charge is fixed, a non-perfect efficiency is required to produce fluctuations. For fixed charge, the efficiency divides into two sets, the measured and non-measured. Each set fluctuates equally, but oppositely, relative to the mean. Thus, all the even moments of net charge will have an even reflection symmetry about an efficiency of  $1/2$ , and the odd moments will have an odd symmetry,

$$C_n(1/2 + \delta\alpha) = \begin{cases} C_n(1/2 - \delta\alpha), & n = 2, 4, 6 \dots \\ -C_n(1/2 - \delta\alpha), & n = 3, 5, 7 \dots \end{cases} \quad (22)$$

### III. RECURSIVE TECHNIQUES FOR GENERATING CANONICAL PARTITION FUNCTIONS

For non-interacting particles the canonical partition function can be calculated exactly, or at least to the level that all partitions of  $A \leq A_{\max}$  hadrons are taken into account, with the exact solution being reached with  $A_{\max} = \infty$ . For our case, we conserve three quantities: the electric charge  $Q$ , the baryon number  $B$  and the strangeness  $S$ . For states  $i$  with energies  $E_i$ , the partition function,

$$Z(Q, B, S) = \sum_{i, Q_i=Q, B_i=B, S_i=S} e^{-\beta E_i}, \quad (23)$$

where  $Q_i, B_i$  and  $S_i$  are the discrete values of the conserved quantities for the state  $i$ , can be calculated recursively. The function  $Z_A(Q, B, S)$  refers to the subset of states with  $A$  hadrons,

$$Z(Q, B, S) = \sum_{A \geq 0} Z_A(Q, B, S). \quad (24)$$

The recursive procedure begins with

$$Z_{A=0}(0, 0, 0) = 1, \quad (25)$$

is the canonical partition function of the vacuum. The contribution for a given  $A$ ,  $Z_A(Q, B, S)$ , can be written as

$$Z_A(Q, B, S) = \frac{1}{A} \sum_h z_h Z_{A-1}(Q - q_h, B - b_h, S - s_h), \quad (26)$$

where  $z_h$  is the single-particle partition function for hadron species  $h$ , which has charges  $q_h, b_h$  and  $s_h$ . This was proved in [3], and can be understood by realizing that one can count all the ways to arrange  $A$  hadrons with a given charge by considering all the ways to arrange one hadron multiplied by all the ways to arrange the remaining hadrons. To avoid double counting, a factor of  $1/A$  is applied. For a fixed charge the probability to have  $A$  hadrons is,

$$P(A) = \frac{Z_A(Q, B, S)}{\sum_A Z_A(Q, B, S)} = \frac{Z_A(Q, B, S)}{Z(Q, B, S)}. \quad (27)$$

In practice, the sum over  $A$  is cut off at some  $A_{\max}$ , but in our studies here that cutoff is made large enough that contributions to  $Z$  for  $A > A_{\max}$  are negligible. Thus, once builds the partition function from  $A = 0$  to  $A_{\max}$  one has the partition function for all  $Q, B, S$ .

Once the partition function is calculated one can also calculate the multiplicities and moments of observing specific species. For example, the multiplicity of species  $h$  in a system with charge  $Q, B, S$  is

$$\langle N_h \rangle = z_h \frac{Z(Q - q_h, B - b_h, S - s_h)}{Z(Q, B, S)}. \quad (28)$$

This also provides expressions for the various charges, e.g.,

$$\langle Q \rangle = \sum_h q_h z_h \frac{Z(Q - q_h, B - b_h, S - s_h)}{Z(Q, B, S)}. \quad (29)$$

Spectra can also be calculated

$$\frac{dN_h}{d^3p} = \frac{(2s_h + 1)\Omega}{(2\pi\hbar)^3} e^{-E_h(p)} \frac{Z(Q - q_h, B - b_h, S - s_h)}{Z(Q, B, S)}. \quad (30)$$

Higher moments can also be extracted,

$$\langle N_h N_{h'} \rangle = \delta_{hh'} z_h \frac{Z(Q - q_h, B - b_h, S - s_h)}{Z(Q, B, S)} \quad (31)$$

$$+ z_h z_{h'} \frac{Z(Q - q_h - q_{h'}, B - b_h - b_{h'}, S - s_h - s_{h'})}{Z(Q, B, S)}. \quad (32)$$

It is straightforward to extend this expression to the fluctuation of charges.

These expressions can also be extended to consider non-additive conservation laws. Net isospin conservation of a hadron gas was invoked in [4], i.e. restricting the states to being in an iso-singlet. For quark-gluon states were restricted to being in both an iso-singlet and a color singlet in [5]. For Bose corrections,

$$Z_A(B, Q, S) = \frac{1}{A} \sum_{h,n} z_{h,n} Z_{A-1}(Q - nq_h, B - nb_h, S - ns_h), \quad (33)$$

$$z_{h,n} = (2s + 1) \sum_p e^{-nE_p/T}. \quad (34)$$

For the conditions of a hadron gas in high-energy heavy-ion collisions only pions are significantly affected by quantum degeneracy.

For the case of a single kind of charge, one can see how the recursive method above yields the same result as what one would expect by writing down the partition function for a system with  $(A - Q)/2$  negative charges and  $(A + Q)/2$  positive charges,

$$Z_{A,Q} = \begin{cases} \frac{z^A}{[(A-Q)/2]![(A+Q)/2]!}, & A - Q \text{ is even,} \\ 0, & A - Q \text{ is odd.} \end{cases}, \quad (35)$$

where  $z$  is the partition function of a single charge. One can readily see that this is consistent with the recurrence relations,

$$Z_{A,Q} = \frac{z}{A} \{Z_{A-1,Q-1} + Z_{A-1,Q+1}\} \quad (36)$$

$$\begin{aligned} &= \frac{z}{A} \left\{ \frac{z^{A-1}}{[(A-Q-2)/2]![(A+Q)/2]!} + \frac{z^{A-2}}{[(A-Q)/2]![(A+Q-2)/2]!} \right\} \\ &= \frac{z}{A} \left\{ \frac{z^{A-1}(A-Q)/2}{[(A-Q)/2]![(A+Q)/2]!} + \frac{z^{A-2}(A+Q)/2}{[(A-Q)/2]![(A+Q)/2]!} \right\} \\ &= \frac{z^A}{[(A-Q)/2]![(A+Q)/2]!}. \end{aligned} \quad (37)$$

This result is also equivalent to expectations based on setting reaction rates equal. If one assumes that pairs are created with some rate  $\beta$ , and that they are destroyed with some rate  $\alpha N_+ N_-$ , where  $N_+$  and  $N_-$  are the number of positive and negative charges,  $N_+ + N_- = A$ . Setting the rates equal,

$$\alpha \frac{(A-Q)(A+Q)}{4} Z_{A,Q} = \beta Z_{A-2,Q}. \quad (38)$$

One can not see that if one chooses  $\beta/\alpha = z$  that Eq.s (38) and (35) are consistent.

Indeed, this result satisfies the recurrence relations above. If the net charge is zero, the result is even simpler,

$$\begin{aligned} P(A|Q) &= \frac{Z_{A,Q}}{\sum_A Z_{A,Q}}, \\ P(A|Q=0) &= \frac{z^A}{[(A/2)!]^2} \left\{ \sum_{A=\text{even}} \frac{z^A}{[(A/2)!]^2} \right\}^{-1}. \end{aligned} \quad (39)$$

Aside from the assumptions that  $Q$  is fixed and there exists only one kind of charge, Eq.(??) also requires that Bose and Fermi quantum statistical corrections are negligible, and that the charges come in unit charges. Despite these shortcomings, this picture is useful in that it allows one to see how multiplicities fluctuations are affected by charge conservation in a simple picture.

One can also find  $\omega_M$  by considering an equilibrated system. Here, we first consider an extremely simplified model of a system with only one conserved charge, and where the species all have charge of either  $-1$  or  $+1$ . Again, the partition functions are labeled by the charge  $Q$  and by the net number of hadrons  $A$ . Because particles have charges only of  $\pm 1$ , the partition function for  $z = Z_{A=1,Q=1} = Z_{A=1,Q=-1}$  forms the basis of all other partition functions. From the methods of the previous section

$$Z_{A,Q} = \frac{z}{A} [Z_{A-1,Q-1} + Z_{A-1,Q+1}]. \quad (40)$$

This relation rapidly reproduces the partition function for all  $A$  and  $Q$  for  $A$  of the order of a few hundred.

#### IV. GENERATION OF UNCORRELATED SAMPLE EVENTS

Complicated experimental acceptances are difficult to incorporate into expressions for the moments. It is then easiest to generate entire events via Monte Carlo, and filter the events through the acceptance. The Monte Carlo procedure involves choosing a hadron proportional the number of ways the system might have such hadron, i.e. a product of the partition function of the individual hadron multiplied by the partition function of the remainder. The procedure becomes:

1. Calculate and store the partition function,  $Z_A(Q, B, S)$ , up to some size  $A \leq A_{\max}$  for all  $Q, B, S$  that might ultimately couple back to a given  $A = A_{\max}$  for the given total values  $Q, B, S$ .
2. For total charge  $Q, B, S$ , choose the number of hadrons  $A$  proportional to  $Z_A(Q, B, S)/Z_A(Q, B, S)$ .
3. Choose a hadron  $h$  proportional to the probability  $z_h Z_{A-1}(Q-q_h, B-b_h, S-s_h)/Z_A(Q, B, S)$ . If Bose degeneracy is to be taken into account this procedure is slight modified as described in Sec. ??.
4. Choose the momentum proportional to the thermal weight  $e^{-E_p/T}$ .

5. Repeat (3,4) but with  $A, Q, B, S$  being replaced by  $A - 1, Q - q_h, B - b - h, S - s_h$ . The procedure is finished when  $A = 0$ .

Bose effects for pions can be included by altering the second and third steps above. In addition to choosing a hadron, one might also consider adding a 2-pion, 3-pion or  $n$ -pion state. Simply treat the  $n$ -pion state as if it were a resonance with charges  $nq_h, nq_b, nq_s$ , but with a partition function  $z_{h,n}$  described above. If one chooses to make such a “particle”, the  $n$  identical particles are given the same momentum and spin projection, using a Boltzmann distribution with a temperature  $T/n$ . To be more realistic the momenta should be smeared by some momenta  $\approx \hbar/R$ , where  $R$  is a characteristic size of the system. If Fermi effects were to be included, one could calculate the partition function by adding a factor  $(-1)^{n-1}$  to each term in the sum described in Eq. (33). However, because some of the weights are negative, Monte Carlo procedures can become problematic. Fortunately, for the systems considered here are extremely hot, and degeneracy of fermions is negligible.

Storing the partition function can require substantial memory for larger  $A_{\max}$  because the indices  $Q, B$  and  $S$  must also vary over a range of order  $\pm A_{\max}$ , so memory usage roughly scales with  $A_{\max}^4$ . Because one is usually interested in calculations with total charge near zero, one can ignore partition functions for charges that cannot couple back to the fixed overall charge at  $A_{\max}$ . Once  $A$  exceeds  $A_{\max}/2$ , the calculations here cutoff values of  $Q, B$  and  $S$  that could not ultimately affect the  $Q = B = S = 0$  partition function for  $A = A_{\max}$ . Even with this savings, partition functions with  $A_{\max} = 250$  could require approximately 13 GB of memory, and need on the order of 10 minutes to calculate on a single processor. For  $A_{\max} = 125$ , less than a GB of memory was needed and partition functions could be calculated in less than a minute. For hadron gases at temperatures of 150 MeV,  $A_{\max} = 250$  was readily sufficient for patch volumes  $\lesssim 700 \text{ fm}^3$ . If multiple patch volumes are to be explored for the same temperature, computational time can also be saved by realizing that the partition functions scale as  $\Omega^4$ . Thus, if one performs a calculation for some initial volume  $\Omega_0$ , scaling can provide results for new volumes with minimal computation.

Once the partition function is calculated, event generation is remarkably fast. The time to generate an even scales linearly with the volume, or equivalently, linear with the average number of particles generated. Running sufficient events to generate a million individual particles can be accomplished within a few seconds on a single CPU. Unlike Metropolis methods where events are modified by considering small changes to existing events, such as in [], each event in this is independent as long as the random numbers are without correlation.

## V. BOSE AND FERMI STATISTICS

Including Bose and Fermi statistics in calculating the partition functions is straight-forward, and was shown in []. The method is related to that used for calculating the effects of multi-boson interference for pion interferometry. In a fixed volume the partition function can be first treated as the usual procedure of accounting for  $n$  identical particles being in different single-particle states. This includes the  $1/n!$  term to account for the fact that particles are indistinguishable, i.e. the Gibbs paradox. If  $m_\ell$  indistinguishable particles are in the same single-particle state  $\ell$ , one must correct the weight by a factor of  $m_\ell!$  for each level, which can also be thought of as the analog of the symmetrized relative wave function with all the momenta being equal. For fermions, the weight becomes  $(-1)^{\ell-1} m_\ell$ . As demonstrated in [], the recurrence relation to the partition function then becomes

$$Z_A(Q, B, S) = \frac{1}{A} \sum_h \sum_n Z_{A-n}(Q - nq_h, B - nb_h, S - ns_h) z_{h,n} (\pm 1)^{n-1}, \quad (41)$$

where  $z_{h,n}$  is the partition function for  $n$  particles in any level,

$$z_{h,n} = \sum_\ell e^{-n\beta(\epsilon_\ell - \mu_i q_i)}. \quad (42)$$

The  $\pm 1$  refers to bosons or fermions. For hadron gases in the high temperature environments of relativistic heavy ion collisions, only pions have a non-negligible correction from quantum degeneracy. The correction for order  $n$  for any level  $\ell$  is of the order  $e^{-\beta(\epsilon_\ell - \mu_i q_i)}$  lower than the previous term. This factor is largest for zero momentum, and for pions becomes  $e^{-\beta(m - \mu)}$ . The chemical potential is  $\mu_Q q_i$  if the pions are chemically equilibrated, but if the system is not chemically equilibrated  $\mu$  is adjusted to fit the average pion density. For the zero-momentum level at a temperature of 150 MeV, the factor is  $e^{-m/T} \approx 0.4$ , and as the system cools probably falls slightly [?]. For a more characteristic thermal momentum the factor is  $\approx 0.1$ . For heavier particles the factor is always small. For example, for a zero-temperature  $\rho$  meson the factor is a fraction of a percent.

Given that symmetrization is only being applied to pions, which are bosons, one can incorporate these corrections into the Monte Carlo procedure outlined in Sec. IV. For fermions this might be problematic because of the negative weights coming from the  $(-1)^{(n-1)}$  factors in Eq (41). Here, the algorithm is adjusted by treating each value of  $n$  as being a different species, with charges  $nq_h$  and with the partition function calculated with a reduced temperature

$T \rightarrow T/n$ . If one picks such a species in step 3 of the algorithm,  $n$  pions are generated, all with the same momentum. For a finite system, the pions would have a small relative momentum or order the inverse system size.

It is well known that bosonic effects can broaden multiplicity distributions [? ], making them super-Poissonian. One of the goals of this study is to discern how bosonic statistics alter the kurtosis or skewness.

## VI. MODELS WITH UNIFORM EFFICIENCY AND FIXED CHARGE

Even for a volume of fixed charge, finite efficiency and acceptance leads to non-zero fluctuations. The degree to which these fluctuations affect the skewness and kurtosis was worked out in [1] for emission of a fixed charge where the probability of any charge being observed was a constant  $\alpha$ . If  $\alpha$  were zero or unity, there would be no fluctuations, and because the charge on those particles that are not observed must fluctuate exactly opposite to the charge that is observed, the even moments must be symmetric about  $\alpha = 1/2$ , and the odd moments must be anti-symmetric. One of the most important results of [1] is that for fixed  $Q$  and  $\alpha$  the ratios cumulants depends only on  $\alpha$  and the variance and mean of the underlying multiplicity distribution. Even though  $Q$  is fixed, the net number of charged particles  $M$  can fluctuate.

From [1], the probability that  $N$  charged particles with total charge  $Q$  will result in a measured charge  $q$  due to a uniform efficiency  $\alpha$  is the convolution of two binomial distributions

$$P(q|M, Q) = \sum_{n_+=0}^{(M+Q)/2} \sum_{n_-=0}^{(N-Q)/2} \frac{[(M+Q)/2]![(M-Q)/2]!}{[(M+Q)/2 - n_+]![(M-Q)/2 - n_-]!n_+!n_-!} \alpha^{n_++n_-} (1-\alpha)^{M-n_+-n_-}. \quad (43)$$

After some tedious algebra, one can find the cumulants for fixed multiplicity,

$$\begin{aligned} C'_1 &= \bar{q} = \alpha Q, \\ C'_2 &= \langle (q - \bar{q})^2 \rangle_M = \alpha(1-\alpha)M, \\ C'_3 &= \langle (q - \bar{q})^3 \rangle_M = \alpha(1-\alpha)(1-2\alpha)Q, \\ C'_4 &= \langle (q - \bar{q})^4 \rangle_M - 3\langle (q - \bar{q})^2 \rangle_M^2 \\ &= \alpha(1-\alpha) - 6\alpha^2(1-\alpha)^2 M. \end{aligned} \quad (44)$$

Here, the primes emphasize that the averages  $\langle \dots \rangle_M$  denote that they consider only those events with fixed base multiplicities  $M$ . The even moments are all linear in  $M$ , while the odd moments are linear in  $Q$ . It might appear that due to the linearity one might replace  $M$  with  $\langle M \rangle$  for a fluctuating base multiplicity, but the second term in the fourth cumulant

$$-3 \sum_M P(M) \langle (q - \bar{q})^2 \rangle_M^2 \neq -3 \langle (q - \bar{q})^2 \rangle^2. \quad (45)$$

Instead,

$$\langle (q - \bar{q})^2 \rangle^2 = \alpha^2(1-\alpha)^2 \bar{M}^2. \quad (46)$$

This provides a contribution to  $C_4$  and the cumulants and their ratios become [1],

$$\begin{aligned} C_1 &= \alpha Q, \\ C_2 &= \alpha(1-\alpha) \bar{M}, \\ C_3 &= \alpha(1-\alpha)(1-2\alpha)Q, \\ C_4 &= \alpha(1-\alpha) - 6\alpha^2(1-\alpha)^2 \bar{M} \\ &\quad + 3^2 \alpha(1-\alpha)^2 \langle (M - \bar{M})^2 \rangle, \\ \frac{C_2}{C_1} &= (1-\alpha) \frac{\bar{M}}{Q}, \\ \frac{C_3}{C_1} &= (1-\alpha)(1-2\alpha), \\ \frac{C_3}{C_2} &= (1-2\alpha) \frac{Q}{\bar{M}}, \\ \frac{C_4}{C_2} &= 1 + 3\alpha(1-\alpha)(\omega_M - 2), \\ \omega_M &\equiv \frac{\langle (M - \bar{M})^2 \rangle}{\bar{M}}. \end{aligned} \quad (47)$$



The relative variance of the multiplicity of the base distribution,  $\omega_M$ , is unity for a Poissonian distribution. In that case  $C_3/C_1$  and  $C_4/C_2$  fall below unity for non-zero  $\alpha$ . The only assumptions for this relation are that the charge is fixed and that the efficiency is uniform. This is important as it implies that if one understands the efficiency and the second moment of the base multiplicity distribution, one can construct a baseline of cumulant ratios, and attribute any deviation from the baseline as due to fluctuations in  $Q$ , which is precisely the goal.

A reasonable value of  $\alpha$  can be taken from balance function analyses. If a charge is observed, there should be a balancing charge emitted nearby, and detected with probability  $\alpha$ . This should correspond to the integrated strength of the charge balance function, which for electric charge is in the neighborhood of 0.4. Of course,  $\alpha$  is not a constant. If a charge is observed in the center of the detector, its balancing charge has a better chance of being observed than for one observed near the periphery of the acceptance. Nonetheless, for the purposes of roughly setting expectations, this suggests that  $C_4/C_2$  can be significantly differ from unity.

Equation (47) is crucial as it demonstrates that the fourth moment of the charge distribution is determined completely by the efficiency and the relative variance of the base multiplicity distribution, if the total base charge  $Q$  is fixed. Next, we consider how various effects, aside from fluctuating the base charge  $Q$ , might push  $\omega_M$  to be either super-Poissonian,  $\omega_M > 1$  or sub-Poissonian. We discuss the effects of volume fluctuations, equilibrated charge distributions, decays and Bose condensation.

### A. Volume Fluctuations

Experiments measure a variety of events of heavy ion collisions, which cover a range of impact parameters. Even for a fixed impact parameter, energy deposition might significantly vary depending on how many nucleons actually collided or how many jets were produced. If more energy is deposited into a fixed volume, it might expand further before it hadronizes, resulting in larger final volumes. Experimental analyses attempt to minimize these fluctuations by constraining a given fluctuation measurement to a specific centrality bin, where “centrality” might be defined by multiplicity, transverse energy, or energy deposition in a forward calorimeter. To reduce auto-correlation centrality measurements are usually constrained to particles other than those used to construct the moments. Nonetheless, it is inevitable that a range of initial conditions is explored within any bin, and one might thus expect the base multiplicity distribution to broaden.

However, as seen in Eq. (47), if the base charge  $Q$  is fixed this affects the result only through the relative variance,  $\omega_M$ , of the base multiplicity distribution, which can be determined by the first and second moments of the multiplicity analysis. For example, the ratio  $C_4/C_2$  reported by STAR for electric charge fluctuations is  $\gtrsim 2$ , which requires  $\omega_M \gtrsim 3$ , which would suggest volumes would have to fluctuate over a range of a factor of two or more in a given centrality bin. Indeed, the centrality bins applied by STAR were not particularly narrow, but unfortunately STAR has not provided the corresponding value of  $\omega_M$  to best gauge the impact of volume fluctuations on the result. Further, it is odd to see that whereas  $C_4/C_2 \gtrsim 2$  for charged particles, it mainly stays below unity for net protons. Thus, the larger values of  $C_4/C_2$  reported by STAR suggest that the source might be true variations in the base distributions of  $Q$ . Phase transitions are usually posed as a means to separate baryon number, much more so than electric charge, so having  $C_4/C_2$  large for net charge, but low for net protons seems to go against the rough expectations presented here for fixed charge, and also against the expectations one might have for fluctuations derived from phase transitions.

### B. Chemically Equilibrated Distribution

One can also calculate  $\omega_M$  for an equilibrated system of a single type of charge, where the measurement directly samples the equilibrated distribution. This ignores decays, which in later stages proceed without the regeneration needed to maintain equilibrium. The results of the equilibrated canonical ensemble in Eq. (39) can be used to find  $\omega_M$ , and thus generate the moments using Eq. (47). For large average multiplicities,  $\bar{M}$ , the value of  $\omega_M$  approaches unity, the Poissonian limit. For small  $\bar{M}$  it approaches two. This is expected, because for a fixed charge, you can only add particles pair-wise. In fact, as will be shown in the next section, if one generated a Poissonian number of pairs, the relative variance would be  $\omega_M = 2$  for all multiplicities. With  $\omega_M$  near unity for any system of significant size the values of  $C_4/C_2$  and  $C_3/C_1$  stay below unity as shown in Fig. 1.

### C. Decays

In addition to the results from the canonical ensemble, a system of uncorrelated neutral particles that decays to charged particles is also presented to illustrate the difference in how charge conservation manifests itself in fluctuation

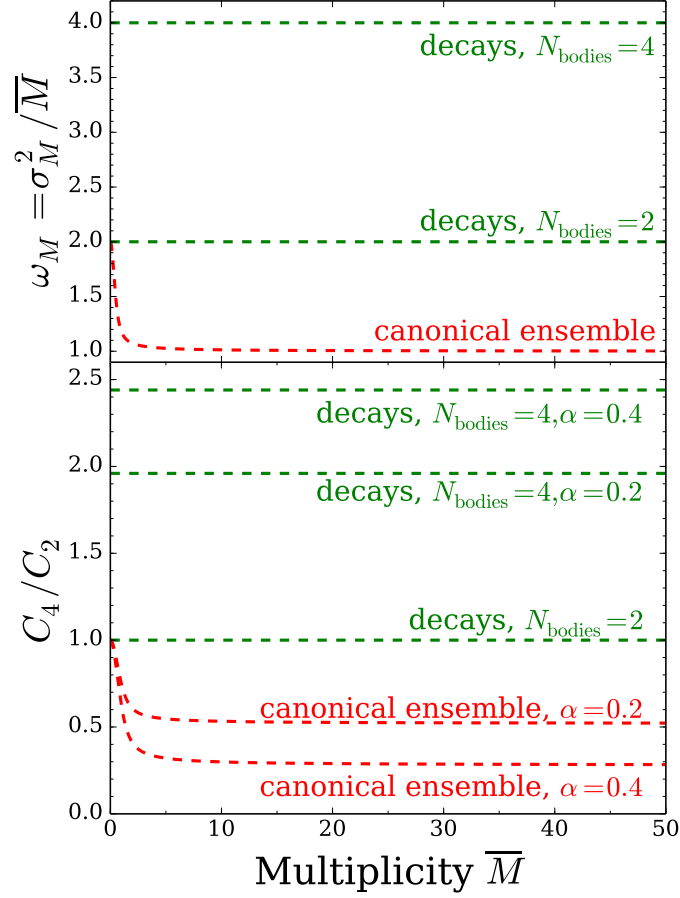


FIG. 1. The relative variance of the charged multiplicity distribution is shown for three cases in the upper panel for a system carrying only a single type of unit  $\pm$ unit charge. For a neutral equilibrated system  $\omega$  approaches the Poissonian limit for higher mean multiplicities,  $\bar{M}$ . This contrasts to a system where one has a Poissonian distribution of neutral particles which all decay into pairs. In this case  $\omega = 2$  and if the number of charged particles coming from the decay,  $N_{\text{bodies}}$ , of the neutral decay were  $n$ , one would have  $\omega = n$ . Using Eq. (47) from [?] the ratio  $C_4/C_2$  is plotted for the cases above for different fixed efficiencies  $\alpha$ . For  $\omega < 2$ ,  $C_4/C_2$  falls below unity, and for  $\omega > 2$  the ratio exceeds unity. The difference from unity is strongest for  $\alpha$  near  $1/2$ , and the result is symmetric for reflecting  $\alpha$  about  $1/2$ . For  $\alpha$  approaching zero or unity  $C_4/C_2 \rightarrow 1$ .

observables depending on whether the charges arise directly from an equilibrated system, or whether they arise from the decays of uncorrelated neutral particles. Here, the multiplicity of the uncorrelated neutral particles is assumed to be Poissonian. If each neutral particle decays into  $N_{\text{bodies}}$  charged particles, where the charges are  $\pm 1$ , the charged particle multiplicity distributions become

$$\begin{aligned} \langle M_{\text{ch}} \rangle &= N_{\text{bodies}} \bar{M}_0, \\ \langle (M_{\text{ch}} - \bar{M}_{\text{ch}})^2 \rangle &= N_{\text{bodies}} \langle (M_0 - \bar{M}_0)^2 \rangle, \end{aligned} \quad (48)$$

$$\omega_M = \frac{\langle (M_{\text{ch}} - \bar{M}_{\text{ch}})^2 \rangle}{\bar{M}_{\text{ch}}} \quad (49)$$

$$= N_{\text{bodies}} \frac{\langle (M_0 - \bar{M}_0)^2 \rangle}{\bar{M}_0}. \quad (50)$$

Fig. 1 illustrates how this picture affects  $C_4/C_2$ . In this case, because  $\omega$  depends only on  $N_{\text{bodies}}$  and does not change with multiplicity or system size, the cumulants are also independent of multiplicity. For  $N_{\text{bodies}} = 2$  the cumulant ratios does not even depend on the efficiency. For  $N_{\text{bodies}} > 2$  the ratio  $C_4/C_2$  exceeds unity, so if charge creation proceeded through the creation and decay of neutral clusters it would be easy to generate large values of  $C_4/C_2$ .

In an equilibrated system decays and recombination have equal rates. However, as the system decouples recombination stops and decays proceed until only stable hadrons remain. Very few decays proceed via more than one charged pair. During the hadronic phase the number of charged particles nearly doubles due to these decays. Thus, if the

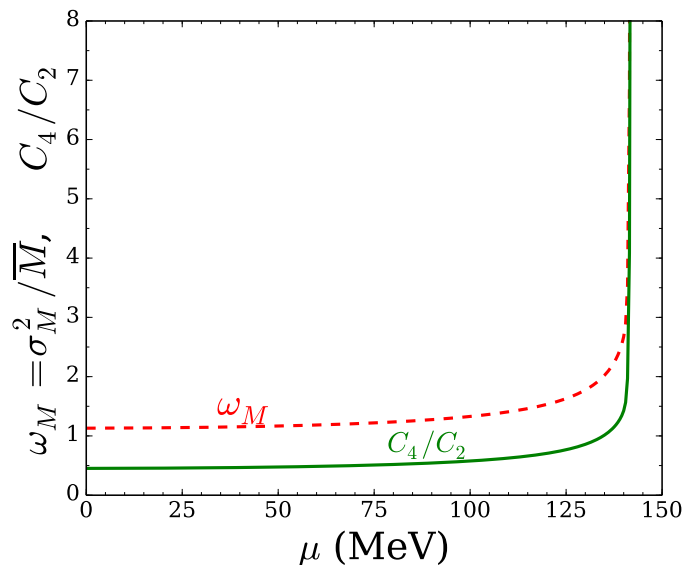


FIG. 2. Fluctuations for a canonical ensemble at fixed charge,  $Q = 0$ , with an effective chemical potential,  $\mu$ , applied to adjust the net pion number in a volume of  $500 \text{ fm}^3$  at a temperature of 100 MeV. The relative variance of the multiplicity distribution (dashed red line) and the ratio  $C_4/C_2$  of the net-charge distribution (solid green line) grow dramatically as  $\mu$  approaches the pion mass. Super-radiant effects can take place once  $\mu$  reaches  $m_\pi = 139.57 \text{ MeV}$ . Heavy-ion collisions are expected to decouple with effective chemical potentials near 75 MeV, which is well below the onset of large fluctuations.

systems do equilibrate, then decay after chemical freeze-out, one would expect the ratio  $C_4/C_2$  to lie somewhere between the value for the canonical ensemble in Fig. 1 and the value for pure decays with  $N_{\text{bodies}} = 2$ . STAR's experimental results for net proton fluctuations indeed satisfy this expectation, but their measured  $C_4/C_2$  for net charge fluctuations well exceed unity. This discrepancy could be due to volume fluctuations or the decay of larger clusters, or perhaps some shortcoming in this overly simple picture, e.g. the neglect of other conservation laws or Bose condensation.

#### D. Bose correlations

It has long been understood that Bose correlations induce super-Poissonian fluctuations. Here, we illustrate how Bose effects combine with charge conservation to determine  $C_4/C_2$ . Partition functions for a gas of positive and negative pions,  $m_\pi = 139.57 \text{ MeV}/c^2$ , were considered to be kinetically equilibrated but with a chemical potential enforcing a fixed average density. If a gas is created at chemical equilibrium one expects  $\mu = 0$ , but if it cools while maintaining a fixed number of pions, and if the pion number is fed by decays, a non-zero value of  $\mu$  is expected. At decoupling one expects kinetic temperatures to fall near 100 MeV and the pion chemical potential to grow to perhaps 75 MeV [6]. This estimate can be understood by the fact that the phase space occupancies should stay roughly constant for fixed entropy per particle for a fixed number expansion, which suggests a chemical potential of approximately 50 MeV by the time the system cools to 100 MeV. Decay products can then further feed the phase space occupancy. Pion condensation occurs when this chemical potential reaches the pion mass. In the absence of Bose effects, this requires roughly doubling the phase space density of pions. However, once such conditions are set Bose effects can result in super-radiance [1], which should be accompanied by large multiplicity fluctuations.

As a function of the effective chemical potential  $\mu$ , the partition function for a pion gas in a volume of  $500 \text{ fm}^3$  and at a temperature of 100 MeV was calculated from Eq. (41). For  $\mu$  in the range of 75 MeV the relative variance of the charged multiplicity distribution is  $\omega_M \approx 1.2$ , which modestly increase  $C_4/C_2$  as shown in Fig. 2 for a fixed efficiency of  $\alpha = 0.3$ . More dramatic results for  $C_4/C_2$  are not expected unless the chemical potential would get within a few MeV of the pion mass. As described above, this is not expected. However, if the number of pion sources fluctuated wildly from one event to another, and if there were some events with twice the number of sources emitting into the same phase space, super-radiance might occur in some small fraction of the events. Such behavior would strongly contradict expectations based on chemical equilibrium.

## E. Hadron Gas

Thus far, all the simple examples presented in this section considered a system with one type of conserved charge, whereas a hadron gas obeys the conservation of baryon number, strangeness and electric charge. This invalidates the use of the recurrence relation of Eq. (47) and requires the application of Eq. (26), or if Bose corrections are included, Eq. (33). Here, we calculate the canonical ensemble,  $Z_A(Q, B, S)$ , using the recurrence relation, then apply the Monte Carlo techniques of Sec. IV to generate sample sets of particles. The calculation is based on a large number,  $\sim 300$ , hadron resonances listed in [? ]. After generating the particles, unstable resonances are decayed. For this section, a uniform efficiency is assumed, independent of species, momenta, or whether the products came from a weak decay (charged pions and kaons were not decayed).

## VII. BLAST WAVE MODEL AND COMPARISON TO STAR RESULTS

## VIII. SUMMARY

## ACKNOWLEDGMENTS

This work was supported by the Department of Energy Office of Science through grant number DE-FG02-03ER41259 and through grant number DE-FG02-87ER40328.

- 
- [1] M. Tanabashi *et al.* [Particle Data Group], Phys. Rev. D **98** (2018) no.3, 030001 doi:10.1103/PhysRevD.98.030001
  - [2] O. Savchuk, R. V. Poberezhnyuk, V. Vovchenko and M. I. Gorenstein, Phys. Rev. C **101** (2020) no.2, 024917 doi:10.1103/PhysRevC.101.024917 [arXiv:1911.03426 [hep-ph]].
  - [3] D. Oliinychenko, S. Shi and V. Koch, arXiv:2001.08176 [hep-ph].
  - [4] S. Pratt and S. Das Gupta, Phys. Rev. C **62**, 044603 (2000) doi:10.1103/PhysRevC.62.044603 [nucl-th/9903006].
  - [5] S. Cheng and S. Pratt, Phys. Rev. C **67**, 044904 (2003) doi:10.1103/PhysRevC.67.044904 [arXiv:nucl-th/0207051 [nucl-th]].
  - [6] S. Pratt and J. Ruppert, Phys. Rev. C **68**, 024904 (2003) doi:10.1103/PhysRevC.68.024904 [arXiv:nucl-th/0303043 [nucl-th]].
  - [7] C. Greiner, C. Gong and B. Muller, Phys. Lett. B **316** (1993), 226-230 doi:10.1016/0370-2693(93)90317-B [arXiv:hep-ph/9307336 [hep-ph]].
  - [8] S. Pratt, Phys. Lett. B **301** (1993), 159-164 doi:10.1016/0370-2693(93)90682-8
  - [9] S. Pratt, E. Sangaline, P. Sorensen and H. Wang, Phys. Rev. Lett. **114**, 202301 (2015).
  - [10] S. Pratt, W. P. McCormack and C. Ratti, Phys. Rev. C **92**, 064905 (2015).
  - [11] J. E. Bernhard, J. S. Moreland, S. A. Bass, J. Liu and U. Heinz, Phys. Rev. C **94**, no. 2, 024907 (2016).
  - [12] J. E. Bernhard, P. W. Marcy, C. E. Coleman-Smith, S. Huzurbazar, R. L. Wolpert and S. A. Bass, Phys. Rev. C **91**, no. 5, 054910 (2015).
  - [13] K. M. Burke *et al.* [JET Collaboration], Phys. Rev. C **90**, no. 1, 014909 (2014).
  - [14] Y. He, L. G. Pang and X. N. Wang, arXiv:1808.05310 [hep-ph].
  - [15] Y. Xu, J. E. Bernhard, S. A. Bass, M. Nahrgang and S. Cao, Phys. Rev. C **97**, no. 1, 014907 (2018).
  - [16] M. Greif, J. A. Fotakis, G. S. Denicol and C. Greiner, Phys. Rev. Lett. **120**, 242301 (2018).
  - [17] S. Pratt, arXiv:1908.01053 [nucl-th].
  - [18] S. Borsanyi, Z. Fodor, S. D. Katz, S. Krieg, C. Ratti and K. Szabo, JHEP **1201**, 138 (2012).
  - [19] G. Aarts, C. Allton, A. Amato, P. Giudice, S. Hands and J. I. Skullerud, JHEP **1502**, 186 (2015).
  - [20] A. Amato, G. Aarts, C. Allton, P. Giudice, S. Hands and J. I. Skullerud, Phys. Rev. Lett. **111**, no. 17, 172001 (2013).
  - [21] G. Policastro, D. T. Son and A. O. Starinets, JHEP **0209**, 043 (2002).
  - [22] J. Casalderrey-Solana and D. Teaney, Phys. Rev. D **74**, 085012 (2006).
  - [23] J. Ghiglieri, G. D. Moore and D. Teaney, JHEP **1803**, 179 (2018).
  - [24] M. Greif, C. Greiner and G. S. Denicol, Phys. Rev. D **93**, no. 9, 096012 (2016) Erratum: [Phys. Rev. D **96**, no. 5, 059902 (2017)]
  - [25] J. Hammelmann, J. M. Torres-Rincon, J. B. Rose, M. Greif and H. Elfner, Phys. Rev. D **99**, no. 7, 076015 (2019).
  - [26] S. Pratt and C. Plumberg, to appear in Phys. Rev. C, arXiv:1812.05649 [nucl-th].
  - [27] C. Shen, Z. Qiu, H. Song, J. Bernhard, S. Bass and U. Heinz, Comput. Phys. Commun. **199**, 61 (2016)
  - [28] S. Pratt, J. Kim and C. Plumberg, Phys. Rev. C **98**, no. 1, 014904 (2018).
  - [29] H. Wang, Ph.D. Thesis, arXiv:1304.2073 [nucl-ex].
  - [30] B. I. Abelev *et al.* [STAR Collaboration], Phys. Lett. B **690**, 239 (2010).  
N. Li *et al.* [STAR Collaboration],
  - [31] J. Adams *et al.* [STAR Collaboration], Phys. Rev. Lett. **90**, 172301 (2003).

- [32] M. M. Aggarwal *et al.* [STAR Collaboration], Phys. Rev. C **82**, 024905 (2010).
- [33] B. Abelev *et al.* [ALICE Collaboration], Phys. Lett. B **723**, 267 (2013).
- [34] C. Alt *et al.* [NA49 Collaboration], Phys. Rev. C **76**, 024914 (2007).
- [35] L. Adamczyk *et al.* [STAR Collaboration], Phys. Rev. C **94**, no. 2, 024909 (2016).
- [36] L. Adamczyk *et al.* [STAR Collaboration], Phys. Rev. C **88**, no. 6, 064911 (2013).
- [37] B. I. Abelev *et al.* [STAR Collaboration], Phys. Rev. Lett. **103**, 251601 (2009).
- [38] S. A. Bass, P. Danielewicz and S. Pratt, Phys. Rev. Lett. **85**, 2689 (2000).
- [39] S. Pratt, Phys. Rev. Lett. **108**, 212301 (2012).
- [40] Y. Pan and S. Pratt, Phys. Rev. C **89**, no. 4, 044911 (2014).
- [41] J. Steinheimer, J. Aichelin, M. Bleicher and H. Stöcker, Phys. Rev. C **95**, no. 6, 064902 (2017).
- [42] J. Steinheimer, J. Aichelin and M. Bleicher, Phys. Rev. Lett. **110**, no. 4, 042501 (2013).